

Characterization of plasma contacts to cadmium telluride photodetector in ultrathin gas discharge cell

Sh.B. Utamuradova¹, Z. Khaydarov^{2*}, B.Z. Khaydarov³

¹Scientific research institute of Physics of semiconductors and microelectronics under the National University of Uzbekistan, Yangi almazar str. 20, Tashkent 100057, Uzbekistan

²Fergana State University, Murabbiylar str. 19, Fergana 150100, Uzbekistan

³Fergana Polytechnic Institute, Fergana str. 86, Fergana 150100, Uzbekistan

email: zokir_nursuh@mail.ru

Abstract

In the present work, the physical properties at the contact of single crystal cadmium telluride semiconductor with gas discharge plasma have been investigated. It is shown that charge carriers in the plasma, together with incident infrared radiation, contribute to the enhancement of the photocurrent in the gas discharge cell. At sufficiently high voltages (more than 2.5 kV) in the gas discharge cell, positive feedback associated with the effect of the plasma on the semiconductor surface is observed. The results of theoretical calculations and experimental experience are in satisfactory agreement, from which the physical meaning of the proportionality coefficient is determined, taking into account the plasma effect on the photoconductivity of the photodetector. The use of a double plasma contact contributes to the damping of the spatial instabilities of the photocurrents in the gas discharge cell, allowing the use of low-resistance photodetectors at the input of the device. Similar results at room temperature have been obtained for the first time on the basis of single-crystal cadmium telluride.

Keywords: gas discharge cell, tellurium cadmium, gas discharge plasma, photoconductivity, photoelectric hysteresis, infrared photography.

PACS numbers: 95.85.Bh , 72.20.-i

<i>Received:</i> 16 September 2024	<i>Revised:</i> 18 October 2024	<i>Accepted:</i> 22 October 2024	<i>Published:</i> 26 December 2024
---------------------------------------	------------------------------------	-------------------------------------	---------------------------------------

1. Introduction

The ultrathin gas discharge cell is a poorly understood object. Nevertheless, the gas discharge cell has found its application in infrared photography [1-9]. Over time, the physical properties of a thin gas discharge cell with various semiconductor electrodes have been studied [10-24].

In particular, in [25, 26] the gas discharge cell with two metal electrodes as well as with one metal and one semiconductor electrode has been studied. It is shown that the voltametric characteristic with two metal electrodes has a strictly vertical character. Lacing of the gas discharge current and luminescence are observed. When one of the electrodes in the gas discharge cell is a semiconductor, the lacing of the current and luminescence disappears, and a uniform luminescence is observed over the entire area of the gas gap.

In [27], the dynamics of the Townsend discharge in the semiconductor gas discharge gap (SGD- structure) was studied when the system is filled with argon. The dependence of the resonant frequency of the structure on the gas discharge current density was studied, as well

as the dependence of the characteristic relaxation time of the discharge on perturbations of the gas discharge gap length for room and low temperatures. The authors describe that the resonant frequency of the structure grows proportional to $\frac{1}{2}$ the gas discharge current, and also the characteristic relaxation time has a superlinear dependence on the gas discharge gap length.

In [28, 29], the physical processes of dissipative structures found in the gas discharge of a gas discharge gap with a semiconductor electrode were described. They observed dissipative structures in the form of hexagonal, trigonal and other types when the length of the gas discharge gap is from 0.3 to 1.0 mm.

In [30] the results of the study of the physical mechanism of gas discharge stabilization by a high semiconductor electrode are presented. Different variants of the gas discharge gap were investigated: A) the semiconductor electrode faces the gap with a free surface; B) the semiconductor surface facing the gap is covered by a continuous metallic nickel layer; C) the semiconductor surface facing the gap is covered by a system of metallic point electrodes. In this case, the thickness of the gas gap was 40 - 70 μm . The voltametric characteristic of the gas discharge gap between the metal electrode and the free surface of the semiconductor is characterized by a smooth increase in current with increasing voltage, a uniform discharge glow is observed. In case B), a stationary current is established in the gas discharge gap at a voltage of more than 600 V, a traveling cord over the electrode surface is observed. In case C), bright spots are observed over the electrode area.

However, the full picture of the physical processes taking place in a thin (40÷100 μm) gas discharge cell is not fully known, especially with respect to practical applications in the field of infrared photography. In [31, 32], we presented theoretical calculations of current kinetics studies in a thin gas discharge cell with two plasma contacts. In the present work, experimental results of the current kinetics of a thin gas discharge cell with two plasma contacts and a cadmium telluride electrode are presented and compared with theoretical calculations.

2. Experiments

The experimental setup was based on a semiconductor photographic ionization chamber (SPIC) [2, 3]. The observed object was an IR monochromator slit with a *NaCl* prism and a light source of the “globar with a ferrite rod” type. The image of the slit was projected by a *BaF₂* lens onto the receiving surface of a cadmium telluride photodetector in a gas discharge cell. The intensity of the radiation incident on the photodetector was determined by direct measurements with a metrological thermocouple of the LETI type with a sensitivity of 0.72 V/W. The recording element in the gas-discharge cell is a fiber-optic disk with a diameter of 36 mm and a length of 22 mm, coated with a conductive layer of *SnO₂*. The optical disk is connected to the input of the electron-optical converter (EOC) type EP-16 (Russian production), and its output is connected to the input of the video control device (VCD) type EMJEON PRO (South Korean production). The optical signal on the EP-16 screen is transmitted to the computer monitor through the VCD. In this way, signal processing by the computer is provided. The gas discharge cell consists of a monocrystalline cadmium telluride, separated on both sides by thin gas gaps (thickness of each gap – $d = 65 \mu\text{m}$ and air pressure – $p = 0.2 \text{ Tor}$) from a fiber-optic washer with a transparent electrode made of *SnO₂*. The semiconductor wafer was carefully polished on both sides to a state of gloss, there were no mechanical scratches or other microscopic disturbances.

The voltage from the UIP-2 type power supply with special voltage amplifiers is applied from the high-voltage transformer between the semiconductor plate and the fiber-optic disk. The residual air pressure in the gas discharge cell is provided by a vacuum pump. At the output of the fiber optic puck, the invisible optical signal is amplified with the help of EP-16,

and then the VCD converts it into a digital signal. Thus, the IR photographic unit assembled by us has a modernized form with the use of modern devices [2].

3. Results and discussion

Let us consider the simplest case, when the effect of plasma current carriers propagates to the entire depth of the semiconductor. In such a case, carriers cause a homogeneous volume generation proportional to the photocurrent j_{PH} , and also to the photoelectron flux $I = j/e = \xi\mu nE$, where μ – is the mobility of carriers in the semiconductor, n – is the concentration of photocarriers, E – is the electric field strength, ξ – is the proportionality coefficient, the physical meaning of which will be explained below. The change of the concentration of non-equilibrium carriers n with time is described by the equation

$$\frac{dn}{dt} = F - n/\tau + \xi\mu nE \quad (1)$$

where F – is the intensity of the optical generation, τ – is the lifetime of the non-equilibrium carriers.

Let us now consider the kinetics of flux build-up when a rectangular voltage step is applied. The solution of equation (1) under the initial condition ($t = 0, n = F\tau$) is given by the formula

$$n = F/(1/\tau - \xi\mu E)\{1 - \xi\mu E\tau \cdot \exp[-t(1/\tau - \xi\mu E)]\} \quad (2)$$

For $E < 1/\xi\mu\tau$, formula (2) has a stationary solution ($t \rightarrow \infty$).

For $E > 1/\xi\mu\tau$, there is no stationary solution ($n \rightarrow \infty$), and the kinetics of current growth is given by the formula

$$n = F/(\xi\mu E - 1/\tau)[\xi\mu E\tau \cdot \exp(t/\tau)(\xi\mu E - 1/\tau)] \quad (3)$$

describes the unbounded exponential growth of the concentration of non-equilibrium carriers with a time constant decreasing in proportion to the electric field strength.

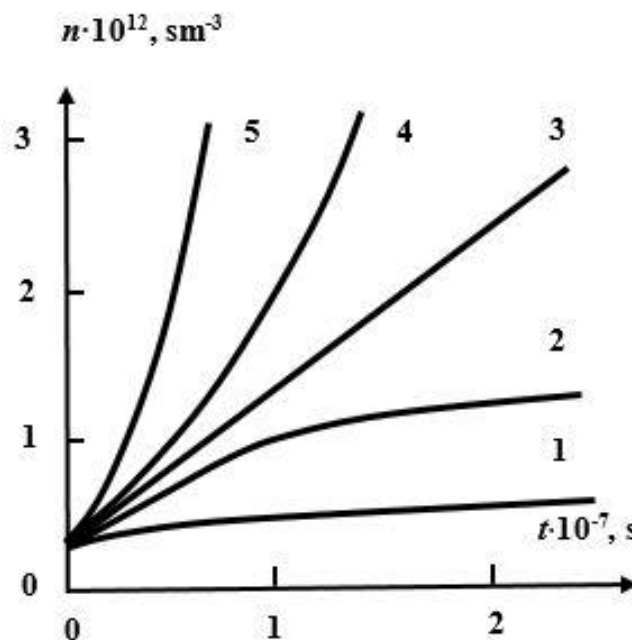


Figure 1. Kinetics of nonequilibrium electron concentration at different values of electric field strength E .

Figure 1 shows the relaxation curves of the non-equilibrium carrier concentration for different values of electric field strength (1 – $E = 5 \cdot 10^3$ V/sm, 2 – $E = 9 \cdot 10^3$ V/sm, 3 – $E = 10^4$ V/sm, 4 – $E = 5 \cdot 10^5$ V/sm, 5 – $E = 5 \cdot 10^6$ V/sm) and optical generation $F = 10^{14}$ sm⁻³s⁻¹, plotted using formulas (2) and (3).

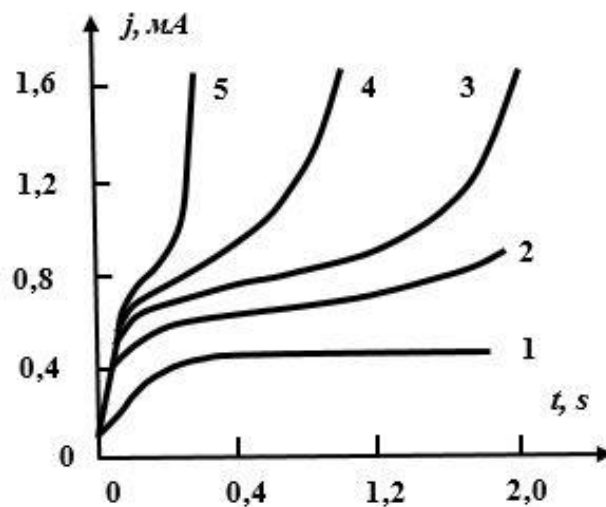


Figure 2. Photocurrent kinetics for different values of the applied voltage on the gas-discharge cell at constant illumination intensity (white light of the order of $4 \cdot 10^{-3}$ Vt/sm²).

Relaxation curves have been recorded for *CdTe* with two plasma contacts in the gas discharge cell, these curves are shown in figure 2 for different values of applied voltage. The voltages are: 1 – 2 kV, 2 – 2.7 kV, 3 – 2.9 kV, 4 – 3 kV and 5 – 3.05 kV.

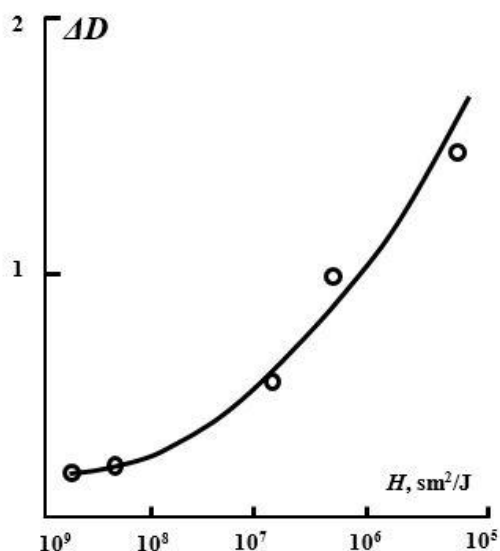


Figure 3. Characteristic curve (absolute value of the optical density of the image from exposure) of the photographic process in SPIC for the spectral wavelength range $\lambda = 2.4 \div 6.9$ μm (enhanced infrared image using an electron-optical converter, operating temperature $T = 80$ K).

Figure 3 shows the characteristic curves of the photographic process with photographic registration of the enhanced image (in the near infrared range) from the screen of the VKU. As follows from the given characteristic curve, the photographic sensitivity is determined by the value of the order $H = 1/(J \cdot t) = 5 \cdot 10^8$ sm²/J. The achieved photographic sensitivity is high

enough. It should be noted that when obtaining the characteristic curves at the inlet of the gas discharge cell, a photodetector made of sulfur-doped silicon [28] and through the gas gap - cadmium tellurium was used. The temperature of the photodetector in the semiconductor photographic ionization chamber (SPIC) was ≈ 80 K. Prior to this work, the operating temperature of this photodetector was at least 60 K to obtain similar results.

From the theoretical calculations (figure 1) it follows that the stationary value of the concentration of nonequilibrium carriers n increases sharply (curve 5) and goes to infinity at $\xi\mu E \rightarrow 1/\tau$. From this condition we can derive the physical meaning of the coefficient ξ . Let us denote $\lambda = 1/\xi$ – some effective length characteristic for the excitation effect of the plasma flux on the semiconductor. Then the condition $\xi\mu E \rightarrow 1/\tau$ can be rewritten as $t = \lambda/\mu E = \tau$ or $\lambda = \mu E \tau$. The greatest effect of plasma excitation occurs when the drift length of carriers in the semiconductor $L_E = \mu E \tau$ becomes equal to λ . In other words, when the transit time t_{ef} of a carrier of characteristic length λ reaches the lifetime $t_{ef} = \tau$ with increasing field strength. If we introduce the carrier transit time of the entire semiconductor length L ($t_{sp} = L/\mu E$), then the condition $\xi\mu E \rightarrow 1/\tau$ can be written as $\tau = (\lambda/L)t_{sp}$. This condition is similar to the exclusion condition ($\tau = t_{sp}$) with the difference that t_{sp} is preceded by the multiplier λ/L , which is the ratio of the characteristic length to the sample length. Thus, ξ is undoubtedly related to the efficiency of the plasma exposure.

The relaxation curves (figure 1) show that at $E = 1/\xi\mu\tau$ the relaxation is characterized by a linear increase of the photocurrent with a slope (curve 3) corresponding to the rate of optical generation rate in the absence of recombination. In this case, recombination losses of carriers are exactly compensated by generation from the plasma and the effective lifetime $1/\tau_{ef} = 1/\tau - \xi\mu E$ – goes to infinity. At $E > 1/\xi\mu\tau$ the condition of negative lifetime condition is realized, the stationary state is absent, there is an exponential-like increase of the photocurrent with time, and positive feedback is observed in the gas discharge cell. In the region $E < 1/\xi\mu\tau$, τ_{ef} is positive, the photocurrent has a stationary value.

As can be seen from the experimental relaxation curves (figure 2), their general character agrees to some extent with the theoretical calculations (figure 1), even in the region of negative lifetimes. For a voltage of 2 kV, the steady state is observed to be reached, and at higher voltages (3.05 kV) a sharp increase in current occurs. However, strong temporal discrepancies in the current kinetics are observed compared to theoretical calculations. This seems to be due to the fact that the simplified calculation did not take into account the peculiar phenomena (it was assumed that the effects of the plasma create uniform non-main carriers throughout the depth of the semiconductor), complex interactions of the plasma carriers of the gas discharge with the surface charges of the semiconductor, and recombination processes. Nevertheless, the results obtained give us a new tool for the application of a thin gas discharge cell with semiconductor electrodes with two plasma contacts for infrared photography, but also for the study of the physical properties of ultrathin gas discharge cells.

As can be seen from the given characteristic curves (figure 3), the photographic sensitivity is determined by the value of the order of $(0.4 \div 0.5) \cdot 10^9$ sm²/J with the amplification on the electron-optical converter. For the above-mentioned spectral range of wavelengths, the obtained photographic sensitivity is high enough. It should be noted that at the same time a sufficiently clear image is visually observed on the EP-16 screen. Achievement of such a result in SPIC at the temperature of 80 K promotes its application in mobile conditions for photodetectors [28].

4. Conclusion

A significant scientific achievement of the present work is that for the first time a damping additional cell (cascade) is used in a gas discharge cell to stabilize the gas discharge, and thus it is possible to advance infrared photography into the far spectral region up to 30 μ m

and beyond. Since now, low impedance photo plates sensitive to infrared radiation can be used at the input stage in a semiconductor photographic ionization chamber. The type of photodetector at the input part of the ultrafine gas-discharge cell does not have, however, any strong influence on the stabilization of the photographic process. However, only the temperature range providing photoelectric hysteresis with photographic (new) effect provides high photographic sensitivity and contrast in a semiconductor photographic ionization cell. Thus, it can be assumed that with similar configurations of electrode arrangement amorphous as well as nanocluster photodetectors with quantum wells for infrared photography at the inlet of a thin gas-discharge cell can be applied sensitive to IR radiation.

From the given characteristic curve, we can conclude that the gas discharge cell with two plasma contacts to the semiconductor is a reliable tool for amplifying the infrared signal with different photodetectors, for example, platinum-doped silicon in the range of 1.2÷4.2 μm and sulfur-doped silicon in the range of 2.4÷6.9 μm .

Acknowledgments

The authors express their gratitude to A.I. Terentyev of the A.F. Ioffe Institute of Physics and Technology of the Russian Academy of Sciences for providing the monocrystalline cadmium telluride.

Authors' Declaration

The authors declare no conflict of interests regarding the publication of this article.

Contribution of the authors

Sh.B. Utamuradova - idea, manuscript preparation; Z. Khaydarov - theoretical calculation, manuscript design; B.Z. Khaydarov - experimental results, drawing design.

References

1. Z. Khaydarov, *UNEC Journal of Engineering and Applied Sciences* **4**(1) (2024) 61.
2. Z. Khaydarov, H.T. Yuldashev, *Applied Physics* **5** (2016) 75. [in Russian]
3. Z. Khaydarov, K.Z. Khaydarova, H.T. Yuldashev, *Applied Physics* **1** (2017) 65. [in Russian]
4. Sh.B. Utamuradova, F.A. Saparov, Z. Khaydarov, *Science and world International scientific journal* **9**(97) (2021) 8. [in Russian]
5. Sh.B. Utamuradova, Kh.S. Daliev, Z. Khaydarov, D.A. Rakhmanov, *Academician: An International Multidisciplinary Research Journal* **11**(9) (2021) 29. [in Russian]
6. L.G. Paritskii, Z. Khaydarov, O. Mukhamadiev, O. Dadabaev, *Semiconductor Physics and Tech.* **27**(11-12) (1993) 2011. [in Russian]
7. Yu.A. Astrov, V.V. Yegorov, Sh.S. Kasymov, V.M. Murugov, L.G. Paritsky, S.M. Ryvkin, Y.M. Sheremetev, *Quantum Electronics* **4**(8) (1977) 1681. [in Russian]
8. H.T. Yuldashev, Sh.S. Kasymov, Z. Khaydarov, *Applied Physics* **2** (2016) 94/ [in Russian]
9. B.G. Salamov, K. Çolakoglu, Ş. Altindal, M. Özer, *Journal de Physique III* **7** (1997) 927.
10. B.G. Salamov, M. Kasap and N.N. Lebedeva, *Journal Applied Physics* **33**(4) (2000) 2192.
11. Yu.A. Astrov, V.B. Shuman, A.N. Lodygin, L.M. Porzel, A.N. Makhova. *Semiconductor Physics and Tech* **42**(4) (2008) 457. [in Russian]
12. M.J. Druyvesteyn, F.M. Penning, *Rev. Mod. Phys.* **12**(2) (1940) 87.
13. B.K. Ridley, *Proc. Phys.* **82**(5) (1963) 954.
14. A.N. Lodygin, L.M. Portsel, Yu.A. Astrov, *Technical Physics* **34**(14) (2008) 61. [in Russian].
15. V.I. Orbukh, N.N. Lebedeva, B.G. Salamov, *Semiconductor Physics and Tech.* **43**(10) (2009) 1329. [in Russian]

16. A.N. Lodygin, L.M. Portsel, Yu.A. Astrov, Letters to Journal of Technical Physics **34**(14) (2008) 61. [in Russian]
17. Yu.A. Astrov, A.N. Lodygin, L.M. Portsel, Journal of Technical Physics **81**(2) (2011) 42. [in Russian].
18. A.N. Lodygin, Yu.A. Astrov, L.M. Portsel, E.V. Beregin, Journal of Technical Physics **85**(5) (2015) 27. [in Russian]
19. T.V. Burova, A.N. Lodygin, L.G. Paritsky, Z. Khaydarov. Russian patent No.0972345 of 22.07.1985. Method of image acquisition in semiconductor ionization photographic system [in Russian].
20. B.G. Salamov, The Imaging Science Journal **21** (2009) 152.
21. B.G. Salamov, T.S. Mammadov, Journal Applied Physics **40** (2007) 6657.
22. B.G. Salamov, N.N. Lebedeva, B.G. Akinoglu, Journal Applied Physics **32** (1999) 2068.
23. Sh.S. Kasymov, L.G. Paritsky, Z. Khaidarov, V.O. Khomidov, S.M. Otazhonov, Physical surface engineering Kharkov **8**(3) 214. [in Russian]
24. H.T. Yuldashev, Z. Khaydarov, Sh.S. Kasymov, Journal of Surface Physics and Engineering **1**(3) (2017) 268. [in Ukrainian]
25. G.M. Sadikh-zade, N.N. Lebedeva, E.A. Sultanov, L.S. Gasanov, Bulletin of Baku University **3** (2005) 1. [in Russian]
26. N.N. Lebedeva, V.I. Orbukh, Ye.Yu. Bobrova, Bulletin of the Azerbaijan National Academy of Sciences **5** (2005) 11. [in Russian]
27. A.N. Lodigin, Y.A. Astrov, L.M. Portsel, E.V. Beregin, Technical Physic **85**(5) (2015) 27.
28. Y.A. Astrov, A.N. Lodigin, L.M. Portsel, Technical Physics **81**(2) (2011) 42.
29. Y.P. Raiser, M.S. Mokrov, Simple physical model of hexagonal current structures in gas discharge with semiconductor cathode, Moscow: Institute of Mechanics Problems of RAS (2009) 47 p. [in Russian]
30. V.I. Orbukh, N.N. Lebedeva, B.G. Salamov, Physics and technology of semiconductors **43**(10) (2009) 1329. [in Russian]
31. H.T. Yuldashev, Z. Khaydarov, Sh.S. Kasymov, Accesses Applied Physics **4**(6) (2016) 580. [in Russian].
32. Z. Khaydarov, H.T. Yuldashev, B.Z. Khaydarov, S. Urmonov, Physical Surface Engineering **13**(2) (2015) 36. [in Russian].